Colloid Polym Sci 274:117–137 (1996)

ORIGINAL CONTRIBUTION

H. Durchschlag
P. Zipper
G. Purr
R. Jaenicke

Comparative studies of structural properties and conformational changes of proteins by analytical ultracentrifugation and other techniques

Received: 3 August 1995
Accepted: 10 August 1995

Dr. H. Durchschlag (✉) · G. Purr
R. Jaenicke
Institute of Biophysics and
Physical Biochemistry
University of Regensburg
Universitätsstraße 31
93040 Regensburg, Germany

P. Zipper
Institute of Physical Chemistry
University of Graz
8010 Graz, Austria

Abstract Analytical ultracentrifugation is a powerful tool for investigating the size of proteins in solution, especially by measuring sedimentation and diffusion coefficients and molar masses. Several further molecular parameters such as frictional ratios, axial ratios of hydrodynamic models, and Stokes radii allow a rough estimate of the protein overall structure. Sedimentation analysis may also be applied efficaciously for monitoring conformational changes of proteins occurring upon ligand binding or denaturation. For the determination of very small changes in shape, however, great care and a series of precautions are required. We investigated the enzymes citrate synthase and malate synthase in the absence and in the presence of ligands, in order to study the structural properties of the proteins and their ligand complexes. We also compared the results of the ultracentrifugal analysis with the results of other solution techniques such as UV absorption, fluorescence spectroscopy, circular dichroism, and small-angle x-ray scattering on the one hand, and the crystallographic 3D structure of citrate synthase on the other. The spectroscopic methods may be used as efficient and rapid tools for screening the occurrence of conformational changes caused by alterations of chromophores and fluorophores. The structural information provided by small-angle scattering (e.g., radii of gyration, maximum particle diameters, volumes and surface areas) can be used to establish quantitative correlations between solution scattering and hydrodynamic data. In this context, however, knowledge or qualified assumptions of partial specific volumes and hydration are additionally required. Good agreement was reached between small-angle scattering and ultracentrifugal data, and also with crystallographic data if protein hydration was considered properly. The given approaches may be used to predict hydrodynamic properties if x-ray data are available, and for many verifications of other structural data, e.g., Stokes radii, diffusion coefficients, axial and frictional ratios determined by independent methods.

Key words Proteins – citrate synthase – malate synthase – analytical ultracentrifugation – small-angle scattering – comparative studies – predictions – structural properties – hydrodynamic modeling – conformational changes

Abbreviations *Materials*: AcCoA, acetyl coenzyme A; CoA, coenzyme A; CS, citrate synthase (EC 4.1.3.7); DTT, dithiothreitol; GdmCl, guanidinium chloride; MS, malate synthase (EC 4.1.3.2). *Methods*: AUC, analytical ultracentrifugation; CD, circular dichroism; EM, fluorescence emission spectroscopy; EX, fluorescence excitation spectroscopy; SAS, small-angle scattering; SAXS, small-angle x-ray scattering; UV, ultraviolet absorption spectroscopy; XD, x-ray diffraction. *Models*: OE, oblate ellipsoidal model; PE, prolate ellipsoidal model.

Colloid & Polymer Science, Vol. 274, No. 2 (1996)

Introduction

The investigation of conformational changes in macromolecules is of particular interest in biochemistry. In the past, sedimentation analysis has often been used to elucidate conformational alterations of the protein structure, frequently neglecting the problems encountered with such investigations, especially in connection with ligand binding and protein stability.

Upon binding specific ligands to proteins, small conformational changes may occur. The investigation of such minute changes by sedimentation analysis is generally accompanied by a number of problems and pitfalls, especially the delicate problem of the separation of the observed effects regarding alterations in mass, anisometry and hydration. In consideration of all these obstacles, the use of additional methods of structural investigation such as spectroscopy or small-angle scattering is advisable.

Large conformational changes, which may occur upon unfolding, dissociation or aggregation of proteins, are relatively easy to detect but often accompanied by problems of interpretation, especially if various changes occur simultaneously. Sedimentation analysis, therefore, is frequently restricted to the mere registration of conformational alterations without further analyzing the individual contributions of mass, anisometry and hydration. Because of the complexity of effects, also in this case the use of additional methods including sedimentation equilibrium is recommended.

In the following, conformational changes of the enzymes citrate synthase and malate synthase upon ligand binding are considered as representative examples. The two enzymes have been studied by analytical ultracentrifugation, spectroscopic techniques (UV, fluorescence, CD) and small-angle x-ray scattering (SAXS). In the case of citrate synthase, the 3D structure has been solved at high resolution, and distinct differences between open and closed forms of the enzyme were characterized by x-ray crystallography [1, 2]. The respective structural changes in solution will be discussed making use of the previously mentioned techniques. In the case of citrate synthase, we also studied the denaturation of the enzyme at extremes of pH, and at varying concentrations of guanidinium chloride, and urea. Subunit dissociation at exceedingly low protein concentration was investigated using malate synthase.

Besides the determination of shapes and shape changes, we strived for finding quantitative correlations between the results observed by hydrodynamic analyses and solution scattering. Among the above mentioned two classes of techniques, analytical ultracentrifugation and small-angle scattering are the most powerful methods in order to characterize the overall protein structure in solution. Useful parameters are sedimentation and diffusion coefficients on the one hand, and the radius of gyration, surface area and volume on the other, apart from molar mass estimations. Moreover, in an attempt to obtain a full account of available structural information, it would be highly desirable to elaborate a link to the results derived from x-ray crystallography. For example, the radius of gyration and the volume are properties which may be calculated from the 3D structure, in addition to the possibility to calculate a theoretical small-angle scattering curve from the atomic coordinates, thereby allowing to compute all molecular parameters normally obtainable from experimental SAXS curves. This obviously provides a fundamental basis for combining the results from hydrodynamic analyses, solution scattering and crystallography.

Attempts to predict hydrodynamic parameters such as sedimentation and diffusion coefficients or Stokes radii have been reported previously [3–11]; they were based either on empirical formulae or on well-founded consierations.

Comparative investigations of protein structures in solution necessitate modeling of their overall structure. Hydrodynamic modeling has a long tradition (e.g., [12–14]) and attracted new attention only recently [15–22]. Modeling proteins, including complex multisubunit structures, based on small-angle scattering data, has also been well known for many years (cf. [23, 24]).

For the comparative analysis of data, we followed Kumosinski and Pessen [25–27] and others (e.g., [28, 29]) who successfully combined hydrodynamic and x-ray data. For a more detailed analysis of structural properties and structural alterations in response to changes in ligation, we included the information from many other sources (cf. Section "Calculations and predictions of hydrodynamic data"). As will be shown, a fair agreement between analytical ultracentrifugation, small-angle scattering, and crystallographic data can be reached if appropriate hydrational contributions are taken into account.

Materials and methods

Materials

Pig-heart citrate synthase (CS) was purchased from Boehringer–Mannheim. For AUC and spectroscopic experiments, the enzyme was dialyzed against a 0.1 M Tris/HCl buffer pH 8.0. For SAXS studies, varying amounts of aggregates present in the stock solution of the enzyme were removed by size-exclusion chromatography (Sephadex G-100); subsequently, the enzyme was concentrated by ultrafiltration and dialyzed against buffer containing 0.2 mM DTT.

Malate synthase (MS) was isolated from baker's yeast and assayed as described previously [30]. Before use, the enzyme was dialyzed against 5 mM Tris/HCl buffer pH 8.1 with 10 mM $MgCl_2$, 1 mM MgK_2EDTA and 0.2 mM DTT. For some AUC and spectroscopic experiments the DTT concentration was raised to 1 mM, and several other stabilizing agents (salts) were added to increase the ionic strength of the solvent. For assays and repair experiments, enzyme solutions with varying DTT concentrations were used.

All reagents were of analytical grade. Quartz bidistilled water was used throughout.

Analysis of structural changes

Ligands, denaturants and other additives were dissolved in the above buffers and their pH was carefully readjusted if necessary. After some time of incubation with these additives (> 30 min), registration was started. References contained the same amounts of additives. Incubations with ligands were performed at 4 °C, while for incubations with denaturants room temperature was used.

Due to the different sensitivity of the techniques used, quite different enzyme and ligand concentrations had to be used. Small-angle x-ray scattering experiments were performed with enzyme concentrations between 2 and 60 mg/ml in the absence/presence of 20 mM oxaloacetate, 50 or 90 mM glyoxylate or pyruvate, 2 or 6 mM AcCoA [31–33]. By contrast, ultracentrifugal and spectroscopic investigations used significantly lower concentrations (cf. Table 3 and [30, 34, 35]). The amount of ligands necessary for sufficient binding was calculated from the respective binding constants (e.g., [30, 36]). Further details are given in the references, figure legends and tables.

All structural investigations were performed at about 4 °C, while a temperature of 25 °C was maintained for the optical test.

Analytical ultracentrifugation

Sedimentation velocity/diffusion and equilibrium experiments were performed in a Beckman model E centrifuge equipped with Schlieren optics and a high-sensitivity ultraviolet scanner system and 10-inch recorder. Sedimentation coefficients were calculated from logarithm of radial distance r vs. time t diagrams. For diffusion coefficients the height-area method was applied. Molar mass determinations made use of the Svedberg equation or sedimentation equilibrium runs applying the meniscus-depletion technique [37].

Small-angle scattering

For SAXS experiments a Kratky camera and copper radiation were used. The analysis and interpretation of SAXS data were performed using theories and methods described [23, 24]. For details with respect to the specific enzymes, see [31, 33, 38]. For the comparative analysis of the data, some additional parameters such as surface areas were determined by reevaluating previous data.

Use of crystallographic data

Using the x-ray diffraction (XD) data of the open and closed forms of CS dimers (absence or presence of oxaloacetate), theoretical SAXS curves were computed on the basis of the Debye formula. Calculations were based either on the coordinates of nonhydrogen atoms (files PDB1CTS and PDB4CTS of the Brookhaven Protein Data Bank), or on the coordinates of the centers of gravity of the amino acid residues. Water molecules and ligands were not included in the calculations. For further details see [33].

Spectroscopy

A Zeiss DMR 10 spectrophotometer was used for measurements of enzymatic activity and UV absorption. Fluorescence studies were performed in Perkin–Elmer MPF-2A or MPF-44A spectrofluorometers. CD spectra were recorded in a Roussel–Jouan Dichrographe II or a JASCO J-500A spectropolarimeter equipped with a DP-500N data processor.

Viscometry and densimetry

Viscosities and/or densities of the solvents are required for AUC and SAXS studies. Viscometric determinations made use of an Ostwald viscometer (5 ml, flow time for water about 325 s). Flow times t were converted to relative viscosities η_{rel}, using $\eta_{rel} = \eta_s/\eta_w = t_s\rho_s/t_w\rho_w$ where subscripts s and w refer to (mixed) solvent and water [39]. Density measurements were carried out using a Paar digital density meter (cf. [40]).

Calculations and predictions of hydrodynamic data

General relations

The calculation of the parameters from AUC experiments (sedimentation and diffusion coefficients, s and D, molar

mass from sedimentation/diffusion and sedimentation equilibrium, $M_{s,D}$ and M_{SE}, respectively) was performed as described in the literature [41–43]. The estimation of further parameters and the prediction of hydrodynamic data from other kinds of information require knowledge of several further relations which were mainly extracted from the pertinent literature. To obtain a uniform calculation scheme, however, most equations had to be adapted appropriately.

The correction of sedimentation coefficients, s (in s), and diffusion coefficients, D (in cm^2/s), to standard conditions (water, 20 °C) may be performed according to (cf. [39, 44, 45]):

$$s_{20,w} = s_{t,s}\left(\frac{\eta_{t,w}}{\eta_{20,w}}\right)\left(\frac{\eta_{t,s}}{\eta_{t,w}}\right)\left(\frac{1-\bar{v}_{20,w}\rho_{20,w}}{1-\bar{v}_{t,s}\rho_{t,s}}\right), \quad (1)$$

$$D_{20,w} = D_{t,s}\left(\frac{\eta_{t,w}}{\eta_{20,w}}\right)\left(\frac{\eta_{t,s}}{\eta_{t,w}}\right)\left(\frac{293.15}{273.15+t}\right), \quad (2)$$

where η denotes the solvent viscosity (usually determined as relative viscosity), ρ the solvent density (in g/cm^3), and $\bar{v}$ the partial specific volume of the macromolecule (in cm^3/g); the subscripts w and s stand for water and any other solvent, respectively, whereas subscript t symbolizes the temperature (in °C) of the experiment. Problems in connection with multicomponent solutions are discussed elsewhere [45].

Usually, $s_{20,w}$ and $D_{20,w}$ values are only corrected for the influence of temperature and the viscosity of the solvent, neglecting smaller corrections such as the temperature dependency of $\bar{v}$ and/or the small influence of ligands on the values of η, ρ, and $\bar{v}$. As will be shown, a rigorous interpretation of conformational changes, reflected by small changes in $s_{20,w}$, however, requires the strict adoption of all terms in the above Eq. (1).

In addition, $s_{20,w}$ and $D_{20,w}$ values have to be extrapolated to $c \to 0$ to eliminate the influence of the concentration dependency of these quantities. In the following, for convenience, the symbols s and D are generally used instead of $s^\circ_{20,w}$ and $D^\circ_{20,w}$.

The Stokes–Einstein equation provides the basis for the derivation of a number of useful molecular parameters such as diffusion coefficient, viscosity and Stokes radius (cf. [10]):

$$D = \frac{kT}{6\pi\eta R_0} = \frac{2.1429\times10^{-6}}{R_0}, \quad (3)$$

where k is the Boltzmann constant, η the viscosity of the solvent in $g\cdot cm^{-1}\cdot s^{-1}$ and R_0 the Stokes radius (rigid-sphere model) in nm. The constant on the right-hand side of Eq. (3) exhibits the unit $cm^2\cdot nm\cdot s^{-1}$.

Frictional ratios, f/f_0, were obtained from different combinations of s, D and M [44]:

from s and M:

$$\frac{f}{f_0} = \frac{1}{\eta(162\pi^2N^2)^{1/3}}\cdot\frac{M^{2/3}(1-\bar{v}\rho)}{s\bar{v}^{1/3}} = 1.1968\times10^{-15}\frac{M^{2/3}(1-\bar{v}\rho)}{s\bar{v}^{1/3}}, \quad (4)$$

from D and M:

$$\frac{f}{f_0} = \left(\frac{4\pi N}{3}\right)^{1/3}\frac{RT}{6\pi\eta N}\cdot\frac{1}{D(M\bar{v})^{1/3}} = \frac{2.9171\times10^{-5}}{D(M\bar{v})^{1/3}}, \quad (5)$$

from s and D:

$$\frac{f}{f_0} = \frac{1}{\eta}\left(\frac{R^2T^2}{162\pi^2N^2}\right)^{1/3}\cdot\left(\frac{1-\bar{v}\rho}{D^2s\bar{v}}\right)^{1/3} = 1.0061\times10^{-8}\left(\frac{1-\bar{v}\rho}{D^2s\bar{v}}\right)^{1/3}, \quad (6)$$

with s, D, and M given in s, cm^2/s, and g/mol, respectively, and the units for the corresponding constants in Eqs. (4–6), $cm\cdot s\cdot mol^{2/3}\cdot g^{-1}$, $cm^3\cdot mol^{-1/3}\cdot s^{-1}$, and $cm^{7/3}\cdot g^{-1/3}\cdot s^{-1/3}$, respectively, and N is Avogadro's number.

In order to consider the effects of protein hydration, the partial specific volume $\bar{v}$ in the above formulae has to be replaced with the hydrated partial specific volume, $\bar{v}_h$ (cf. [46, 47]):

$$\bar{v}_h = \bar{v}_2 + \delta_1\bar{v}_1, \quad (7)$$

where $\bar{v}_2$ and $\bar{v}_1$ symbolize the partial specific volume of protein and water, while δ_1 stands for the protein hydration (g of water per g of protein). Equation (7) does not apply to $\bar{v}$ when used in the buoyancy term.

The molar mass of proteins was estimated from s or D and the intrinsic viscosity $[\eta]$, given in cm^3/g, according to:

from s and $[\eta]$:

$$M = \frac{1}{10}\left(\frac{N\eta}{\beta}\right)^{3/2}\cdot\frac{s^{3/2}[\eta]^{1/2}}{(1-\bar{v}\rho)^{3/2}} = 1.483\times10^{22}\frac{s^{3/2}[\eta]^{1/2}}{(1-\bar{v}\rho)^{3/2}}, \quad (8)$$

from D and $[\eta]$:

$$M = 100\left(\frac{\beta kT}{\eta}\right)^3\cdot\frac{1}{[\eta]D^3} = \frac{6.582\times10^{-14}}{[\eta]D^3}, \quad (9)$$

based on the concepts derived by Flory, Mandelkern and Scheraga ([4, 5], cf. [44]). For the parameter β, a value of $2.15\times10^6\,mol^{-1/3}$ was chosen. The constants in Eqs. (8) and (9) have the units $g^{3/2}\cdot cm^{-3/2}\cdot s^{-3/2}\cdot mol^{-1}$ and $cm^9\cdot s^{-3}\cdot mol^{-1}$, respectively.

Employing the Stokes–Einstein equation and considerations by Polson [3, 6] and Young, Carroad and Bell [8], several further estimations of molar masses can be given:

$$M = \left(\frac{A}{D}\right)^3 , \tag{10}$$

where A is a constant with the value of 2.74×10^{-5} $cm^2 \cdot s^{-1} \cdot g^{1/3} \cdot mol^{-1/3}$ [3];

$$M = \frac{1}{[\eta]} \cdot \left(\frac{B}{D}\right)^3 , \tag{11}$$

where B is a constant with the value of 4.19×10^{-5} $cm^3 \cdot s^{-1} \cdot mol^{-1/3}$ [6];

$$M = \left(\frac{8.34 \times 10^{-10} T}{\eta D}\right)^3 = \left(\frac{C}{D}\right)^3 , \tag{12}$$

where the constant C has a value of 2.44×10^{-5} $cm^2 \cdot s^{-1} \cdot g^{1/3} \cdot mol^{-1/3}$ [8]. Obviously, the Young–Carroad–Bell method (Eq. (12)) yields an expression similar to Eq. (10) given by Polson [3], and the Polson Eq. (11) resembles Eq. (9).

Empirical equations, relating M of globular proteins and s or R_0 (derived from D via Eq. (3)), respectively, were established by Squire and Himmel [7] and were improved by Dang and Dang [9]:

$$M = 2.159 \times 10^{23} s^{3/2} , \tag{13}$$

$$M = 1770 R_0^3 , \tag{14}$$

where s has to be given in s and R_0 in nm, the constants having the units $g \cdot mol^{-1} \cdot s^{-3/2}$ and $g \cdot mol^{-1} \cdot nm^{-3}$, respectively.

Evidently, applying a given value for M, predictions for s, D and R_0 are possible making use of the above-mentioned relations (cf., e.g., [10]).

Recent considerations by Tyn and Gusek [10] provided a further predictive method for D of globular particles (proteins, viruses) by combining the Stokes–Einstein equation and the radius of gyration, R_G (a quantity obtainable from light or x-ray solution scattering):

$$D = \frac{1.69 \times 10^{-6}}{R_G} , \tag{15}$$

where the constant has the unit $cm^2 \cdot s^{-1} \cdot nm$ and R_G is given in nm.

Prediction of hydrodynamic parameters from SAXS data

As pointed out by Kumosinski and Pessen [25–27], sedimentation coefficients s of roughly globular molecules (proteins, viruses) may be derived from SAXS parameters (radius of gyration R_G, hydrated volume V, surface-to-volume ratio S/V, axial ratio p).

For the calculation of s values, the following form of the Svedberg equation was used:

$$s = \frac{M(1 - \bar{v}\rho)}{(f/f_0)\, 6\pi\eta N R_0} = 8.7919 \times 10^{-17} \frac{M(1 - \bar{v}\rho)}{(f/f_0)\, R_0} , \tag{16}$$

where M is the anhydrous molar mass (for proteins preferably obtained from the amino acid sequence or composition), $\bar{v}$ the partial specific volume of the macromolecular solute (preferably experimental), ρ and η are the density and viscosity of water at 20 °C, respectively. The constant on the right-hand side of Eq. (16) has the unit $nm \cdot s \cdot mol \cdot g^{-1}$.

The Stokes radius R_0 was derived from the hydrated volume V (in nm^3) instead of the commonly used partial specific volume $\bar{v}$:

$$R_0 = \left(\frac{3V}{4\pi}\right)^{1/3} , \tag{17}$$

and the frictional ratio f/f_0 of the hydrated particles was calculated modeling the particles as prolate or oblate ellipsoids of revolution of axial ratio p according to Perrin's formulae [12, 13]:

$$\frac{f}{f_0} = \frac{(p^2 - 1)^{1/2}}{p^{1/3} \ln[p + (p^2 - 1)^{1/2}]} \quad (p > 1, \text{ prolate}) , \tag{18}$$

$$\frac{f}{f_0} = \frac{(1 - p^2)^{1/2}}{p^{1/3} \tan^{-1}[(1 - p^2)^{1/2}/p]} \quad (p < 1, \text{ oblate}) , \tag{19}$$

where p equals c/a, with a designating the equatorial radius of the ellipsoid, and c its semiaxis of revolution. It should be noted that this definition of p is in accord with Luzzati et al. [48] and Kumosinski and Pessen [25–27], but is the reciprocal of the p defined by others (e.g., [16]).

The axial ratios p were obtained by combining R_G with V or S/V of the hydrated particles:

$$\frac{3V}{4\pi R_G^3} = \frac{p}{\left(\frac{p^2 + 2}{5}\right)^{3/2}} \quad (p \lessgtr 1) , \tag{20}$$

and

$$R_G \frac{S}{V} = \frac{3}{2p}\left[1 + \frac{p^2}{(p^2 - 1)^{1/2}} \sin^{-1} \frac{(p^2 - 1)^{1/2}}{p}\right] \times \left(\frac{p^2 + 2}{5}\right)^{1/2} \quad (p > 1) , \tag{21}$$

or

$$R_G \frac{S}{V} = \frac{3}{2p}\left[1 + \frac{p^2}{(1-p^2)^{1/2}} \tanh^{-1}(1-p^2)^{1/2}\right] \times \left(\frac{p^2+2}{5}\right)^{1/2} \quad (p < 1)\,. \tag{22}$$

In the case of the enzyme-ligand complexes, for M and $\bar{v}$ the respective values of the complexes were used in Eq. (16).

Diffusion coefficients D were calculated according to:

$$D = \frac{kT}{(f/f_0)\,6\pi\eta R_0} = \frac{2.1429 \times 10^{-6}}{(f/f_0)R_0}\,, \tag{23}$$

where the constant on the right-hand side of Eq. (23) has the unit $cm^2 \cdot nm \cdot s^{-1}$, and R_0 is given in nm.

Prediction of hydrodynamic parameters from XD data

For prediction of s and D values, the radius of gyration R_G was calculated from the atomic coordinates and electron densities of the crystallographic structure. As volume, the anhydrous volume or, alternatively, an estimated hydrated volume was used (assuming a hydration of $\delta_1 = 0.35$ g/g [47]). The axial ratio p was derived from R_G and V.

Experimental investigation of conformational changes

Problems encountered with the investigation of small conformational changes

For optimum function proteins may be rigid or flexible (cf. [49]). In the case of enzymes, flexibility is important for performing the catalytic reaction, i.e., binding of substrates and release of products. Frequently, the conformational changes are triggered by low-molecular weight ligands, leading to motions of domains (transitions between open and closed conformations; cf. Fig. 1). In order to allow the study of such changes, the enzymes have to be fixed in well-defined conformational states under fixed conditions. This may be accomplished by investigating them either in the absence or presence of specific ligands (substrates, coenzymes, cofactors, products, analogs and diverse combinations), avoiding progress of the catalytic reaction.

In many cases such conformational changes only lead to slight changes of parameters of the overall structure which are accessible to a hydrodynamic or solution scattering analysis. The detection or, even more, the detailed analysis of such small changes encounters many problems,

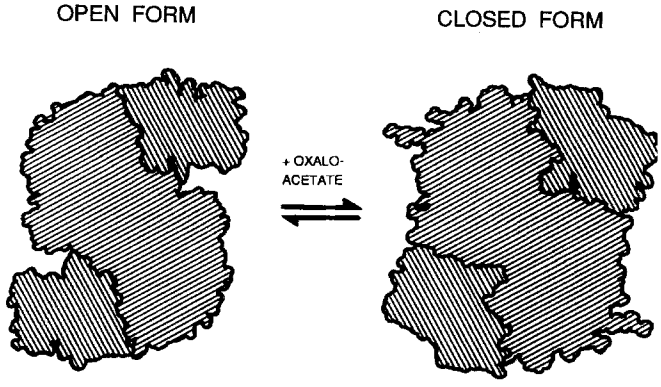

Fig. 1 Schematic drawing of open and closed forms of pig-heart citrate synthase dimers; large and small enzyme domains are differently shaded. The low-molecular weight substrate oxaloacetate is the main trigger of the conformational change. The drawing only shows the protein moieties; it is based on a space-filling model calculated from the atomic coordinates [33, 50]

is prone to many errors, and requires special techniques and evaluation procedures as well as a series of precautions (cf. [33]).

Techniques and evaluative procedures

In principle, numerous physico-chemical techniques are able to detect small conformational changes occurring in proteins as a consequence of ligand binding or other environmental changes. Hydrodynamic techniques (such as AUC and viscometry), chromatographic methods (e.g., size-exclusion chromatography) and solution scattering (such as small-angle x-ray or neutron scattering, light scattering) allow changes of the overall structure in solution to be monitored, thus complementing information obtained from x-ray and neutron crystallography. Further details with respect to the protein structure (changes of intrinsic absorption and fluorescence, preferably of aromatic chromophores and fluorophores, as well as signals from extrinsic labels) become accessible from diverse spectroscopic techniques (UV absorption, fluorescence emission and eΠxcitation, far- and near-UV circular dichroism).

In spite of the large number of techniques, only a few turned out to be suitable for the investigation of small conformational changes, among them AUC, SAS, and the spectroscopic techniques.

By means of AUC, preferably changes of $s_{20,w}$, $D_{20,w}$, and M are followed, whereas SAS exploits alterations of radius of gyration, R_G, radius of gyration of the cross-section, R_C, radius of gyration of the thickness, R_t, molar mass, M, distance distribution function, $p(r)$, and maximum particle diameter, d_{max}, as preferred targets of the

analysis. Among these parameters, $s_{20,w}$ and R_G are most important. However, their changes commonly do not exceed 1–5%.

Special problems and precautions

The most important problems arising in connection with the detection of small conformational changes in proteins are the following:

– Reasonable amounts of pure material (both of protein and ligands) are required (1 μg to 100 mg, depending on the method used).

– For molar mass estimates by means of AUC or SAS, ρ of the solvent and the specific volume of proteins and ligands must be known either by experiment or calculation [40, 51]. The proper correction of sedimentation coefficients to standard conditions also requires precise knowledge of the values for $\bar{v}$ of the protein and η and ρ of the solvent at different temperatures, both in the absence and presence of the various ligands.

– Due to the presence of the ligands and the use of buffer solutions, one deals with multicomponent solutions [52, 53]. Therefore, if possible, the protein together with the ligands has to be dialyzed against the corresponding buffer.

– In connection with AUC experiments, the influence of primary and secondary charge effects should be kept in mind when performing sedimentation runs. Experiments in the absence/presence of ligands in very dilute buffers may give rise to difficulties in the interpretation of data.

– As a consequence of the presence of ligands, the extent of preferential interactions may change, leading to changes of the specific volume of protein, hydration and binding of solvent components (cf. [39, 40, 54]).

– In order to guarantee sufficient binding of ligands, elevated ligand concentrations are required. This may lead to unspecific (unproductive) binding of the ligands. This poses the question of whether any extrapolation should be made to low or high ligand concentrations.

– The instability of samples during the time needed for an AUC or SAS experiment may cause serious problems: Proteins (e.g., sulfhydryl enzymes) may suffer from oxidative damage and labile ligands (e.g., oxaloacetate) may decompose under certain conditions.

– Impurities of samples may disturb a proper analysis of conformational changes.

– Aggregation (due to protein denaturation) may cause artifacts, especially when applying solution scattering techniques. Fractionation of the samples by size-exclusion chromatography may reduce the problem.

– Similarly, the presence of protein fragments (e.g., as a consequence of proteolysis or radiation damage) may blur the interpretation of conformational changes.

– The amount of aggregates or fragments may be influenced by the presence of certain ligands. Generally aggregation is highest for the unliganded protein or in the absence of other additives. Ligands may exhibit a stabilizing effect (e.g., against proteolytic cleavage, inactivation, aggregation, denaturation, radiation damage).

– The occurrence of radiation damages, which again result in aggregation, fragmentation, and alterations of chromophores and fluorophores, etc., is a serious problem for techniques applying UV light or x-rays (e.g., for SAXS studies [31, 33]).

– For the study of small conformational changes, relative measurements under varying conditions (e.g., different amounts of additives) are needed. Many errors cancel out when working under comparable conditions. For the detection of small conformational changes upon ligand binding by means of sedimentation velocity, the substrate-free protein in each run is required as a reference (use of a multihole rotor).

– The interpretation of conformational changes is complicated by the fact that frequently multiple changes may occur simultaneously. A delicate interpretative problem is the separation of the effects due to changes of size and shape of the protein on the one hand and alterations of hydration on the other. In this case SAS experiments are clearly superior to hydrodynamic methods such as AUC.

– To allow a detailed interpretation of conformational changes of the protein moiety upon ligand binding, in principle the contribution of the ligands has to be separated from the overall effects of the protein-ligand complex [38]. This is a sophisticated problem because for its solution the approximate location of the ligand(s) needs to be known. Since generally the mass of the ligand(s) is very low and can often be neglected in relation to the great protein mass, this separation is not applied in most cases.

– A quantitative comparison of the parameters obtained from various techniques is often hampered by differences in the conditions regarding experimental temperature, concentration of protein, ligands and other buffer components (causing different kinds of interactions, shielding and ionic strength effects resulting, for example, in different amounts of aggregates), and use of standardizations. This holds especially when findings from AUC and SAS are to be compared: high concentrations of proteins and ligands are required for SAS, while low concentrations are sufficient for AUC; usually standardizations to water and 20 °C are common for sedimentation coefficients but not for parameters obtained from solution scattering.

Colloid & Polymer Science, Vol. 274, No. 2 (1996)

Probing the extent of large conformational changes

Of course, the same methods which are able to render small conformational changes can be used for investigating larger changes, as caused, for example, by varying amounts of denaturing agents, such as guanidinium chloride, urea, pH, or detergents etc. To mention a few problems only, arising in connection with the evaluation of transition curves: simultaneous occurrence of different species, short-lived intermediates, kinetic perturbations due to slow equilibration, problems of evaluation in classifying spectroscopic signals, etc. The investigation of protein denaturation/folding has been described in detail (see [55–60]).

Structure and function of citrate synthase and malate synthase

For our considerations we used two enzymes of similar function but different subunit structure, namely citrate

Table 1 Characteristics of citrate synthase and malate synthase, respective ligands, and enzyme-ligand complexes[a]

Enzymes	Number of subunits	M (g/mol)	$\bar{v}$ (cm^3/g)	
			4 °C	20 °C
CS	2	97938 (from amino acid sequence) [b] 98300 ± 900 (from SAXS)[e] 96000–105000 (from AUC)[f]	0.733[c]	0.740[d]
MS	3	187000 ± 3000 (from SAXS)[g] 175000–191000 (from AUC)[f]	0.738[g]	0.745[d]

Ligands	M (g/mol)	$\bar{v}$[h] (cm^3/g)	V[h] (nm^3)
$Glyoxylate^-$	73	0.548	0.07
$Pyruvate^-$	87	0.644	0.09
$Oxaloacetate^{2-}$	130	0.477	0.10
$Citrate^{3-}$	189	0.461	0.14
CoA^{3-}	765	0.636	0.81
$AcCoA^{3-}$	807	0.642	0.86

Enzyme-ligand complexes[i]	M[j] (g/mol)	ΔM[j] (%)	$\bar{v}$[k] (cm^3/g)	
			4 °C	20 °C
CS · oxaloacetate	98198	+ 0.27	0.732	0.739
CS · citrate	98316	+ 0.39	0.732	0.739
CS · AcCoA	99551	+ 1.65	0.732	0.738
CS · CoA	99467	+ 1.56	0.732	0.738
CS · AcCoA · oxaloacetate	99811	+ 1.91	0.731	0.738
CS · CoA · citrate	99845	+ 1.95	0.730	0.737
MS · glyoxylate	187220	+ 0.12	0.738	0.745
MS · pyruvate	187260	+ 0.14	0.738	0.745
MS · AcCoA	189420	+ 1.29	0.737	0.744
MS · AcCoA · pyruvate	189680	+ 1.43	0.737	0.744

[a] The table comprises only properties required for the following calculations and considerations. Abbreviations: CS, pig-heart citrate synthase; MS, yeast malate synthase
[b] From [61]
[c] From [62]
[d] Value at 4 °C converted to 20 °C, using $\Delta\bar{v}/\Delta T = 4.5 \times 10^{-4}\ cm^3 g^{-1} K^{-1}$ [54]
[e] This value is based on a reevaluation of data provided by Wilfing [32]
[f] See Table 2
[g] From [31]
[h] Derived from the molar volume $\bar{V}$ which was calculated according to [51]
[i] It is assumed that each enzyme subunit binds only one molecule of each ligand
[j] Calculated on the basis of the above values for enzymes (M = 97938 or 187000 g/mol, respectively) and ligands
[k] Calculated on the basis of the above values for enzymes and ligands, assuming additivity of volumes [40]

synthase and malate synthase (cf. Table 1). Both enzymes have been characterized using different physico-chemical techniques, especially AUC and SAXS, as well as spectroscopic techniques (UV absorption, fluorescence emission and excitation, near- and far-UV circular dichroism). Results are taken from earlier studies [30–35, 38, 63] and more recent evaluations and experiments.

Citrate synthase

Citrate synthase, the primary pacemaker enzyme of the tricarboxylic-acid cycle, catalyzes the condensation between acetyl coenzyme A (AcCoA) and oxaloacetate to form citrate and coenzyme A (CoA). For reviews see: [36, 64–67].

The pig-heart enzyme has been characterized by several physico-chemical investigations, including AUC, SAXS and spectroscopy [32, 33, 62, 68, 69], its 3D structure has been solved to high resolution by x-ray diffraction [1, 2]. The enzyme is a homodimer; each subunit consists of 437 amino acid residues organized in a large and a small domain. The ligands are bound in a cleft between the two domains. The enzyme crystallizes in one open and two closed forms (cf. Fig. 1). The open form represents the substrate binding and product release form. By contrast, the catalytic action of the enzyme only proceeds in the closed form. Both substrates can induce a closed structure, with oxaloacetate being the main trigger of the conformational change. Several compounds may act as analogs (e.g., oxoglutarate, malate, tartrate, succinate, nucleotides like ATP or NADH), however they exhibit only weak binding compared to the true substrates and products.

Though x-ray crystallography showed very clearly rather large conformational changes between open and closed form, early hydrodynamic and spectroscopic techniques had difficulties to detect the corresponding alterations in solution (e.g., [68, 70–73]. However, taking care of the instability of oxaloacetate in aqueous buffer solution, recent SAXS studies succeeded in clearly distinguishing the open and closed forms of the enzyme [33, 63].

Malate synthase

Malate synthase, a key enzyme of the glyoxylic acid cycle, catalyzes the aldol condensation of glyoxylate with AcCoA to yield malate and CoA. The enzyme from baker's yeast has been characterized regarding its enzymological [30, 74, 75], physico-chemical and spectral properties [31, 34]. The physico-chemical measurements include AUC and SAXS; however, so far no crystal structure is available. The enzyme has been described as a trimer of presumably identical subunits. Similar to citrate synthase, both substrates may induce conformational changes, and a series of further ligands (e.g., 2-oxo acids) may act as analogs. Pyruvate has been reported to be a substrate analog to mimic the structural effects of glyoxylate upon ligand binding.

The yeast enzyme is a sulfhydryl enzyme, the integrity of the accessible sulfhydryl residues being essential for catalytic activity and, presumably, for maintaining the native structure [76]. Oxidation of enzyme solutions (e.g., after long-term storage) leads to the formation of disulfides and other oxidation products.

Results and discussion

Structural properties of citrate synthase and malate synthase and conformational changes upon ligand binding

Hydrodynamic parameters of the two unliganded synthases obtained from AUC and viscometric studies are given in Table 2 which summarizes earlier data from the literature and recent unpublished results. Table 3 comprises a set of ultracentrifugal and spectroscopic data of several enzyme-ligand complexes, including results obtained at varying concentrations of additives.

In Table 4 a variety of structural parameters of citrate synthase are summarized. Data derived from SAXS experiments and simulations of SAXS on the basis of crystallographic results are presented both for the unliganded enzyme and the enzyme-oxaloacetate complex. The shape of the enzyme and the complex was modeled by prolate and oblate ellipsoids. Structural parameters of malate synthase and of three enzyme-ligand complexes are given in Table 5. Both the enzyme and its complexes are approximated by oblate ellipsoidal models. Refined models, obtained by elimination of the contribution of the ligands, reflect the shape of the enzyme moiety in the enzyme-ligand complexes.

Predictions of several hydrodynamic parameters of citrate synthase and malate synthase and the respective complexes were performed on the basis of the two sets of data in Tables 4 and 5. Results are presented in Tables 6 and 7.

Finally, in Table 8 the structural changes of the two synthases upon ligand binding are summarized. The table comprises experimental results from two solution techniques (SAXS and AUC) and comparisons between experimental and predicted data (XD and SAXS, SAXS and AUC).

The given results will be discussed in connection with the applied methods, followed by a comparative discussion of the different findings and techniques.

Colloid & Polymer Science, Vol. 274, No. 2 (1996)

Table 2 Hydrodynamic parameters of the unliganded forms of citrate synthase and malate synthase as obtained from AUC and viscometry[a)]

Parameter	CS	MS
Literature Data and New Results:		
$s^0_{20,w}$ (s)	6.0×10^{-13} [62] 6.2×10^{-13} [69]	8.3×10^{-13} [30] $(8.6 \pm 0.1) \times 10^{-13}$ [b)c)]
$D^0_{20,w}$ (cm²/s)	5.8×10^{-7} [62]	4.5×10^{-7} [30] $(4.4 \pm 0.1) \times 10^{-7}$ [b)]
$[\eta]$ (cm³/g)	3.95 [62]	
$M_{s,D}$ (g/mol)	96 000 [62]	175 000 [30] 186 000 ± 5 000 [b)]
M_{SE} (g/mol)	96 000 [69] 100 000 [62]	180 000 [30] 191 000 ± 8 000 [b)]
$M_{s,[\eta]}$ (g/mol)	105 000 [62]	
Estimation of Further Parameters:[d)]		
Frictional ratio f/f_0:[e)]		
from s, M and $\bar{v}$ (Eq. (4))	1.185	1.287
from D, M and $\bar{v}$ (Eq. (5))	1.206	1.279
from s, D and $\bar{v}$ (Eq. (6))	1.199	1.282
$\langle f/f_0 \rangle$	1.197	1.282
Frictional ratio f/f_0:[f)]		
from s, M and $\bar{v}_h$ (Eqs. (4) and (7))	1.041	1.132
from D, M and $\bar{v}_h$ (Eqs. (5) and (7))	1.060	1.125
from s, D and $\bar{v}_h$ (Eqs. (6) and (7))	1.054	1.127
$\langle f/f_0 \rangle$	1.052	1.128
M (g/mol) according to Scheraga and Mandelkern:		
from s and $[\eta]$ (Eq. (8))	107 700	
from D and $[\eta]$ (Eq. (9))	85 400	
$\langle M_{s,[\eta]}, M_{D,[\eta]} \rangle$	96 500	
M (g/mol) according to Polson:		
Eq. (10)	105 400	241 500
Eq. (11)	95 400	
M (g/mol) according to Young, Carroad and Bell:		
Eq. (12)	74 500	170 500
M (g/mol) according to Dang and Dang:		
from s (Eq. (13))	105 400	172 200
from R_0 derived from D (Eqs. (14) and (3))	88 900	204 400
$\langle M_s, M_D \rangle$	97 200	188 300

[a)] Abbreviations: CS, pig-heart citrate synthase; MS, yeast malate synthase

[b)] Since MS turned out to be a sulfhydryl enzyme [76], new experiments were performed in the presence of sufficient amounts of a sulfhydryl reagent (0.2–1 mM DTT) and/or other stabilizing agents. The results for s, D, and M turned out to be slightly different from previous data

[c)] The $s_{20,w}$ was determined at 4 °C and standardized to water and 20 °C, using a temperature correction for $\bar{v}$ [54]. Neglecting the temperature dependence of $\bar{v}$ would yield $(8.8 \pm 0.1) \times 10^{-13}$ s

[d)] The following calculations are based on the currently most reliable values: $s = 6.2 \times 10^{-13}$ s, $D = 5.8 \times 10^{-7}$ cm²/s, $M = 97\,938$ g/mol, $\bar{v} = 0.740$ cm³/g, and $[\eta] = 3.95$ cm³/g for CS; $s = 8.6 \times 10^{-13}$ s, $D = 4.4 \times 10^{-7}$ cm²/s, $M = 187\,000$ g/mol, and $\bar{v} = 0.745$ cm³/g for MS

[e)] These calculations neglect hydration

[f)] These calculations use the hydrated partial specific volume $\bar{v}_h$ (Eq. (7)) instead of the anhydrous partial specific volume $\bar{v}$, assuming a hydration of $\delta_1 = 0.35$ g water per g of protein (cf. [47])

Analytical ultracentrifugation

Making use of AUC experiments, unliganded citrate synthase and malate synthase were characterized by their hydrodynamic parameters s, D and M (Table 2); additional hydrodynamic information was obtained from intrinsic viscosity, $[\eta]$.

Frictional ratios, f/f_0, calculated from different combinations of s, D and M, show good agreement (Table 2), provided the latter quantities are properly determined.

Table 3 Comparison of structural changes of citrate synthase and malate synthase upon ligand binding, as revealed by AUC and spectroscopic techniques[a]

Ligand/ Additive	$c_{ligand/additive}$ (mM)	AUC	UV absorption	Fluorescence		Circular dichroism		
				Emission	Excitation	Near-UV		Far-UV
		$\Delta s^{c}_{20,w}$[b] (%)	$\Delta\lambda_{UV,max}$[c,d] (nm)	$\Delta\lambda_{EM,max}$[c,e] (nm)	$\Delta\lambda_{EX,max}$[c,f] (nm)	$\Delta\theta_{260}$[g] (%)	$\Delta\theta_{295}$[g] (%)	$\Delta\theta_{220}$[h] (%)
Citrate Synthase:								
Oxaloacetate	0.1		−0.5	+ 0.9	+ 0.8			
	0.5		−2.0	+ 1.7	+ 3.3			
	1	+ 1.0	−3.0	+ 1.7	+ 7.3	+ 66	−3	+ 5
	3	+ 1.0	−3.0					
	10	+ 1.5	−3.5					
Citrate	10	0	0	+ 0.4	+ 1.0	+ 39	no change	no change
Tartrate	10		0	+ 0.4	0			
L-Malate	10		−0.5	−0.1	0			
L-Lactate	10		+0.5	−0.1	0			
AcCoA	0.05			+ 0.9	+ 3.5			
	0.1	+ 3.5	−2.0	+ 1.4	+ 5.0	− 31	no change	no change
	0.3	+ 3.5						
	1	+ 4.0						
CoA	0.1			+ 0.4	+ 4.0			
	1	+ 3.5						
AcCoA + oxaloacetate	0.05 + 0.25			+ 1.4	+ 4.0			
	0.05 + 0.5			− 0.1	+ 5.5			
	0.1 + 1	+ 1.5	−2.0					
AcCoA + citrate	0.1 + 10	+ 2.5	−1.0	+ 0.7	+ 4.0	+ 108	no change	
Citrate + oxaloacetate	10 + 0.5			+ 1.4	+ 3.5			
Malate Synthase:[i]								
Glyoxylate	2	−0.4 ± 0.3						
	5	−0.4 ± 0.2						
	10	−1.0 ± 0.3		−6.0		−68	−98	no change
	50	−2.0 ± 0.3		−6.0				
Pyruvate	10	−0.9 ± 0.5		−6.5		−90	−71	no change
	50	−1.9 ± 0.5		−7.0				
AcCoA	0.5	+ 0.6 ± 0.2						
	1	+ 0.8 ± 0.2		+ 1.0		+ 18	− 9	no change
	2	+ 1.0 ± 0.5		+ 1.0				
AcCoA + pyruvate	0.5 + 10	0.0 ± 0.2						
	1 + 10	+ 0.6 ± 0.4		− 5.0		− 344	− 73	no change
	2 + 50	−1.1 ± 0.5		−5.5				

[a] The investigations were performed in the presence of varying concentrations of different additives. Most of these additives may act as ligands (see text); for comparison a few examples of additives not acting as effective ligands are added. Due to the different sensitivity of the various techniques, the protein concentration had to be varied in the experiments. Note: techniques which require higher $c_{protein}$ also need higher $c_{ligand/additive}$ to guarantee sufficient ligand binding. Abbreviations: CS, pig-heart citrate synthase; MS, yeast malate synthase. In the case of MS, relatively high protein concentrations were used to avoid inteference with concentration-dependent effects (see text)

[b] $c_{protein}$ = 0.5 mg/ml (CS) and 2.0 mg/ml (MS); accuracy of Δs, unless otherwise stated: ± 0.5%; $\Delta s_{20,w}$ values are uncorrected for the influence of ligands or different degrees of saturation

[c] Accuracy $\Delta\lambda$: ± 0.5 nm; a positive sign signals a red shift, while a blue shift is indicated by a negative sign

[d] $c_{protein}$ = 0.1 mg/ml (CS); $\lambda_{UV,max}$ = 278.5 nm (unliganded CS)

[e] $c_{protein}$ = 0.01 mg/ml (CS) and 0.5 mg/ml (MS); unliganded CS: $\lambda_{EM,max}$ = 329.1 nm (λ_{EX} = 280 nm); unliganded MS: $\lambda_{EM,max}$ = 331 nm (λ_{EX} = 285 nm)

[f] $c_{protein}$ = 0.01 mg/ml (CS); unliganded CS: $\lambda_{EX,max}$ = 280.0 nm (λ_{EM} = 330 nm)

[g] $c_{protein}$ = 1 mg/ml (CS) and 8 mg/ml (MS); accuracy of $\Delta\theta$: ± 5%

[h] $c_{protein}$ = 0.1 mg/ml (CS) and 0.5 mg/ml (MS); accuracy of $\Delta\theta$: ± 5%

[i] Reevaluated from previous data [34]

The correct interpretation of f/f_0 in terms of shape (axial ratio) requires knowledge (or reasonable assumptions) with respect to protein hydration. Applying such a procedure yields f/f_0 values which are in fair accord with the findings of the more efficient solution x-ray scattering technique (cf. Tables 6 and 7).

The determination of the molar protein masses by several predictive approaches (Table 2) renders slightly

Colloid & Polymer Science, Vol. 274, No. 2 (1996)

Table 4 Structural parameters of citrate synthase obtained from experimental and theoretical SAXS data[a]

Parameter[b]	Experimental[c]		Theoretical[d]	
	Unliganded form	Oxaloacetate complex[e]	Open form	Closed form
R_G (nm)[f]	2.91 ± 0.02	2.80 ± 0.00	2.84	2.74
R_c (nm)[f]	2.12 ± 0.01	2.13 ± 0.01	2.16	2.22
d_{max} (nm)			9.62	8.83
r_{fr} (nm)[f]	3.50 ± 0.01	3.40 ± 0.00	3.45	3.39
V (nm^3)	174 ± 2	164 ± 1	119.9[g]	119.9[g]
δ_1 (g/g)	0.339 ± 0.011	0.274 ± 0.007		
S/V (nm^2/nm^3)	0.884 ± 0.021	0.851 ± 0.025		
V/M (nm^3·mol/g)	(1.78 ± 0.02) × 10^{-3}	(1.67 ± 0.01) × 10^{-3}		
$S/M^{2/3}$ (nm^2·mol$^{2/3}$/g$^{2/3}$)	(7.25 ± 0.19) × 10^{-2}	(6.56 ± 0.20) × 10^{-2}		
Prolate Ellipsoidal Models:[h]				
$a = b$ (nm)	2.86	2.86	2.29	2.36
c (nm)	5.10	4.77	5.46	5.14
p	1.785	1.667	2.387	2.177
S/V (nm^2/nm^3)	0.913	0.921	1.096	1.074
Oblate Ellipsoidal Models:[h]				
$a = b$ (nm)	4.32	4.11	4.36	4.17
c (nm)	2.23	2.31	1.50	1.64
p	0.516	0.562	0.345	0.394
S/V (nm^2/nm^3)	0.941	0.940	1.215	1.157

[a] The experimental parameters in this table are based on a critical reevaluation of data provided by Wilfing [32]. The theoretical parameters were calculated using the crystal data
[b] Explanation of parameters: R_G, radius of gyration; R_c, radius of gyration of the cross-section; d_{max}, maximum particle diameter; r_{fr}, most frequent intraparticle distance; V, particle volume; S/V, surface-to-volume ratio; δ_1, hydration (g of water per g of protein); a, b, c, semiaxes of ellipsoidal models; $p = c/a$, axial ratio
[c] Experiments were performed at 4 °C
[d] The calculated values do not include water molecules and ligands
[e] The values given for the secondary complex contain the contribution of the ligand oxaloacetate
[f] Taken from [33]
[g] Sum of atomic volumes; this value is nearly identical to the anhydrous volume calculated from the partial specific volume according to $V = M \cdot \bar{v}/N$
[h] The volumes of the models are identical to the above-mentioned V values

different results, depending on the parameters used, and the assumptions underlying the used formulae and estimations. In the case of citrate synthase, the results can be checked by comparing with M calculated from the amino acid sequence.

With the sulfhydryl enzyme malate synthase, use of the previously determined values for s, D and M [30] would result in diverging f/f_0 values (not shown), suggesting that earlier determined values are inaccurate, presumably due to insufficient amounts of a protective thiol (cf. Section "Concentration-dependent changes of malate synthase"). The comparison of previous and recent s values (cf. Table 2) with those now predicted (Table 7) supports this assumption.

Sedimentation coefficients of a great variety of enzyme ligand complexes clearly reveal the occurrence of shape changes (Table 3). However, the effects depend significantly on the type of enzyme and the additive, where both the additive itself and its concentration are of importance. In comparing the results quantitatively, the following facts have to be kept in mind: i) The overall sedimentation coefficient is affected by the mass of the ligands. As may be taken from Table 1, the mass contribution of the class of small ligands (2-oxo acids or citrate) amounts only to 0.1–0.4% of the mass of the enzyme, while the mass of the nucleotides (AcCoA, CoA) is much greater (1.3–1.7%), the percentages depending on the protein mass and the number of binding sites. The influence of the mass on the sedimentation coefficient may be estimated roughly from the relation $s \sim M^{2/3}$ (cf. Eq. (13)), indicating a negligible influence of the small ligands, but a considerable effect of AcCoA and CoA. ii) Low ligand concentrations may lead to incomplete ligand binding, depending on the respective binding constant (e.g., MS + 2 mM glyoxylate). iii) High additive concentrations (e.g., MS + 50 mM glyoxylate) require a highly sophisticated correction of the $s_{20,w}$ values (influence of the ligand concentration on η, ρ, and $\bar{v}$, cf. the earlier "General relations" section and Table 8).

Table 5 Structural parameters of malate synthase obtained from experimental SAXS data[a]

Parameter[b]	Unliganded form	Glyoxylate/ Pyruvate complex[c]	AcCoA complex[d]	AcCoA · pyruvate complex[e]
R_G (nm)	3.96 ± 0.02	3.91 ± 0.03	3.93 ± 0.02	3.92 ± 0.02
R_a (nm)	0.99 ± 0.04	1.02 ± 0.04	1.04 ± 0.04	1.00 ± 0.04
d_{max} (nm)	11.2 ± 0.6	10.7 ± 0.3	10.9 ± 0.5	11.0 ± 0.2
V (nm^3)	338 ± 5	338 ± 1	358 ± 5	344 ± 3
δ_1 (g/g)	0.35 ± 0.02	0.35 ± 0.00[f]	0.41 ± 0.02[f]	0.36 ± 0.01[f]
S/V (nm^2/nm^3)	0.80 ± 0.03[g]			
V/M (nm^3 · mol/g)	$(1.81 \pm 0.04) \times 10^{-3}$			
$S/M^{2/3}$ (nm^2 · mol$^{2/3}$/g$^{2/3}$)	$(8.27 \pm 0.36) \times 10^{-2}$			
Oblate Ellipsoidal Models:				
$a = b$ (nm)	6.06	5.96	5.99	5.99
c (nm)	2.21	2.29	2.33	2.23
p	0.364	0.384	0.389	0.372
R_G (nm)	3.96	3.91	3.93	3.92
R_a (nm)	0.99	1.02	1.04	1.00
V (nm^3)	340	341	350	336
δ_1 (g/g)	0.357	0.359[f]	0.382[f]	0.332[f]
S/V (nm^2/nm^3)[h]	0.840	0.824	0.813	0.838
Refined Oblate Ellipsoidal Models:[i]				
$a = b$ (nm)		5.95	5.94	5.93
c (nm)		2.29	2.33	2.22
p		0.385	0.392	0.374
R_G (nm)		3.90	3.90	3.88
R_a (nm)		1.02	1.04	0.99
V (nm^3)		340	344	327
δ_1 (g/g)[j]		0.356	0.371	0.315
S/V (nm^2/nm^3)[h]		0.824	0.815	0.843

[a] Most of the parameters are taken from [31, 38]
[b] Explanation of parameters: R_a, axial radius of gyration (cf. [38]); for other parameters see Table 4
[c] Secondary complex with glyoxylate or pyruvate
[d] Secondary complex with AcCoA
[e] Ternary complex with AcCoA and pyruvate
[f] Evaluated from the given volume after correction for the ligand contributions
[g] Evaluated from mean intersection length given in [31]
[h] Evaluated from the given axes and volumes
[i] The refined models refer to the enzyme moiety in enzyme-ligand complexes; they have been obtained by eliminating the ligand contributions (cf. [38])
[j] Evaluated from the given volumes

Keeping these complications in mind, we may state unequivocally that both synthases show conformational changes of the protein moieties upon ligand binding. Citrate synthase exhibits changes on binding its substrates oxaloacetate and AcCoA, while citrate alone obviously does not result in any structural change. These data are compatible with the findings from crystallography, showing that both substrates may act as triggers for the conformational change to the closed form, while citrate does not appear to induce a conformational change (cf. [50, 66]). The interpretation of the data for the ternary complexes is by far more complicated (if possible at all). In the case of the simultaneous presence of oxaloacetate and AcCoA, the enzymatic reaction proceeds continuously and, as a consequence of the time needed for performing a sedimentation run, the enzyme finally results in a CS · citrate · CoA complex. The formation of such a complex would, at most, give rise to a marginal effect. The investigation of further ligand complexes is hampered by the low affinity of analogs; it would require much higher ligand concentrations, leading to the above-mentioned additional complications.

Malate synthase shows very subtle, but significant changes of its structure upon binding the substrates glyoxylate and AcCoA. The substrate analog pyruvate perfectly substitutes glyoxylate regarding its conformational changes. Therefore, the ternary complex MS · AcCoA · pyruvate

Table 6 Predictions of hydrodynamic parameters of citrate synthase from SAXS and crystal structure data[a)]

Parameter	Unliganded form				Oxaloacetate complex			
R_0 (nm)[b)]	3.47 (3.06) [3.48]				3.40 (3.06) [3.48]			
$D_{R_G} \times 10^7$ (cm^2/s)[c)]	5.81 (5.95) [5.95]				6.04 (6.17) [6.17]			
	PE		OE		PE		OE	
	R_G, V	$R_G, S/V$	R_G, V	$R_G, S/V$	R_G, V	$R_G, S/V$	R_G, V	$R_G, S/V$
p[d)]	1.785 (2.387) [1.593]	1.655	0.516 (0.345) [0.596]	0.597	1.667 (2.177) [1.298]	1.285	0.562 (0.394) [0.759]	0.776
f/f_0[e)]	1.030 (1.070) [1.020]	1.023	1.038 (1.098) [1.024]	1.023	1.024 (1.055) [1.006]	1.006	1.029 (1.076) [1.007]	1.006
$s \times 10^{13}$ (s)[f)]	6.30 (6.88) [6.34]	6.35	6.26 (6.70) [6.31]	6.35	6.51 (7.00)[g)] [6.45][g)]	6.63	6.48 (6.87)[g)] [6.45][g)]	6.63
$D \times 10^7$ (cm^2/s)[h)]	6.00 (6.55) [6.04]	6.04	5.95 (6.38) [6.01]	6.04	6.16 (6.63)[g)] [6.11][g)]	6.27	6.13 (6.51)[g)] [6.11][g)]	6.27

[a)] The underlying experimental SAXS data were obtained at about 4 °C. The values in parentheses and brackets are calculated from crystal structure data and are based on the anhydrous volume or an assumed hydration $\delta_1 = 0.35$ g/g [47], respectively
[b)] The Stokes radius R_0 was calculated via Eq. (17) from the volumes given in Table 4
[c)] The diffusion coefficient D_{R_G} was calculated according to Eq. (15)
[d)] The axial ratio p was calculated either from R_G and V or R_G and S/V, respectively, assuming prolate or oblate ellipsoids (PE, OE) as model shapes for the enzyme (cf. Eqs. (20–22))
[e)] The frictional ratio f/f_0 was computed using Perrin's formulae (Eqs. (18 and 19))
[f)] The sedimentation coefficient s was obtained from Eq. (16)
[g)] The mass and the volume of the ligand were taken into account
[h)] The diffusion coefficient D was derived from Eq. (23)

may mimic the true ternary complex adequately. For a more detailed consideration of the influence of ligands see also Table 8.

Sedimentation runs were paralleled by spectroscopic investigations. However, due to the different sensitivities of the techniques, different concentrations of the protein and its ligands had to be chosen in order to obtain unambiguous results.

Spectroscopic techniques

As may be inferred from Table 3, a plethora of different ligand-induced alterations of the spectroscopic signals were monitored in the UV absorption, fluorescence excitation and emission, and also in the near-UV circular dichroism. There seem to be no changes in the circular dichroic absorption in the far-UV range.

In the case of citrate synthase, there was a small, but significant blue shift (maximum about 3 nm) in the UV absorption spectrum in response to binding the substrates oxaloacetate and/or AcCoA, but not for citrate, tartrate, malate or lactate. UV difference spectra clearly indicated changes in the range of 260 nm (probably due to Tyr) for oxaloacetate, AcCoA, and the ternary complexes. Correspondingly, fluorescence emission spectra revealed minute, but reproducible red shifts (of about 1.5 nm) upon formation of these complexes. The excitation spectra yielded rather large red shifts (5–7 nm). The changes in fluorescence emission and excitation can be ascribed to alterations in the neighborhood of intrinsic fluorophores (Trp and/or Tyr). Similarly, the near-UV CD spectrum shows marked differences due to changes in the environment of the aromatic chromophores, the alterations being quite different for the different ligands. The far-UV CD spectrum revealed no significant differences; obviously, the secondary structure of the enzyme is not affected by ligand binding, in agreement with the considerations by Wiegand and Remington [66].

For the enzyme-ligand complexes of malate synthase, a similar picture emerged as described above for the sedimentation coefficients. Again, glyoxylate and pyruvate

Table 7 Predictions of hydrodynamic parameters of malate synthase from SAXS[a]

Parameter	Unliganded form		Glyoxylate/ Pyruvate complex	AcCoA complex	AcCoA · pyruvate complex
R_0 (nm)[b]	4.32		4.33	4.37	4.31
$D_{R_G} \times 10^7$ (cm^2/s)[c]	4.27		4.33	4.30	4.32
	OE		OE	OE	OE
	R_G, V	$R_G, S/V$	R_G, V	R_G, V	R_G, V
p[d]	0.364	0.395	0.384 (0.385)	0.389 (0.392)	0.372 (0.374)
f/f_0[e]	1.089	1.075	1.079 (1.079)	1.077 (1.076)	1.085 (1.084)
$s \times 10^{13}$ (s)[f]	8.95	9.07	9.03 (9.03)[g]	9.11 (9.12)[g]	9.20 (9.20)[g]
$D \times 10^7$ (cm^2/s)[h]	4.55	4.61	4.58 (4.58)[g]	4.55 (4.55)[g]	4.58 (4.59)[g]

[a] The underlying experimental SAXS data were obtained at about 4 °C. The values in parentheses refer to the refined models presented in Table 5
[b] The Stokes radius R_0 was calculated via Eq. (17) from the volumes given in Table 5
[c] The diffusion coefficient D_{R_G} was calculated according to Eq. (15)
[d] The axial ratio p was calculated either from R_G and V or R_G and S/V, respectively, assuming oblate ellipsoids (OE) as model shapes for the enzyme (cf. Eqs. (20 and 22))
[e] The frictional ratio f/f_0 was computed using Perrin's formula (Eq. (19))
[f] The sedimentation coefficient s was obtained from Eq. (16)
[g] The mass and the volume of the ligand(s) were taken into account
[h] The diffusion coefficient D was derived from Eq. (23)

cause similar effects on the fluorescence emission spectra, whereas those observed for AcCoA and the ternary complex are quite distinct. Near-UV CD spectra exhibit different changes at different wavelengths, with alterations of θ_{295} probably attributable to changes of the environment of Trp residues. The alterations observed for AcCoA alone were marginal, regarding both fluorescence emission and near-UV CD.

Though there is no way of correlating quantitatively the spectroscopic results with hydrodynamic data, spectroscopy may be applied as a useful means for proving the occurrence of conformational changes. Quantitative correlations, however, may be anticipated between ultracentrifugal data and the results of scattering and diffraction studies.

Small-angle scattering

The experimental and theoretical SAXS results for citrate synthase are in fair accord, both with regard to the absolute values and the structural changes upon ligand binding (e.g., decrease of radius of gyration, R_G, and of maximum particle diameter, d_{max}; Tables 4 and 8). According to the experimental results, there is also a pronounced decrease of V, S/V and δ_1. Neither the prolate nor the oblate ellipsoidal model (for short: PE and OE) fit the experimental data satisfactorily, however, the prolate model is clearly superior (as follows, for example, from a comparison of scattering curves). In spite of this deficiency, an increase of isometry upon formation of the enzyme-ligand complex may be concluded (decrease of axial ratio p in case of PE model). The comparison of the models derived from XD data on the one side and SAXS data on the other suffers from inconsistencies of the underlying volumes.

The SAXS investigations of malate synthase and several enzyme-ligand complexes revealed a variety of subtle changes of conformational parameters (e.g., decrease of R_G and d_{max}; Tables 5 and 8). The interpretation of structural changes is complicated by the considerable (non-negligible) mass of the ligand AcCoA. Sophisticated considerations, however, allow a separation of the effects caused by this and the other ligands. This approach leads to "refined models" (Table 5). The structural changes upon forming the ternary complex (enzyme · AcCoA · pyruvate) are more drastic than the changes caused by the binding of a single ligand. They can be interpreted in terms of a volume contraction, decrease of hydration and increase of isometry, similar to the observations with citrate synthase.

Prediction of hydrodynamic parameters from X-ray data

Irrespective of the model used for citrate synthase (PE, OE), similar f/f_0 values and similar predictions for s and D were possible (Table 6). Only slight differences were

Table 8 Comparison of structural changes of citrate synthase and malate synthase upon ligand binding, as revealed by XD, SAXS and AUC[a]

Percent change of parameter	CS[b] Oxaloacetate complex		MS[c] Glyoxylate/ Pyruvate complex	MS[c] AcCoA complex	MS[c] AcCoA · pyruvate complex
X-Ray Analysis:	*XD*	*SAXS*	*SAXS*	*SAXS*	*SAXS*
ΔR_G	−3.5	−3.8	−1.3	− 0.6	− 0.9
			(−1.4)	(− 1.4)	(− 1.9)
ΔR_c or ΔR_a	+ 2.8	+ 0.5	+ 3.5	+ 5.1	+ 1.0
			(+ 3.5)	(+ 5.1)	(0)
ΔV		− 5.7	0	+ 5.9	+ 1.8
			(0)	(+ 1.2)	(− 3.8)
$\Delta\delta_1$		− 19	+ 0.6[d]	+ 7.0[d]	− 7.0[d]
			(− 0.3)	(+ 3.9)	(− 11.8)
Δd_{max}	− 8.2	− 6.5[e]	− 4.5	− 2.7	− 1.8
			(− 1.8)[f]	(− 2.0)[f]	(− 2.1)[f]
Δp from model	− 8.8[g]	− 6.6	+ 5.5	+ 6.9	+ 2.2
	(− 18.5)[h]		(+ 5.8)	(+ 7.7)	(+ 2.7)
Prediction of Hydrodynamic Parameters from X-Ray Data:					
Δs from model (use of R_G and V)	+ 1.8[g]	+ 3.3	+ 0.9	+ 1.8	+ 2.8
	(+ 1.8)[h]				
Δs from model (use of R_G and S/V)		+ 4.4			
AUC Analysis: [i]					
$\Delta s^c_{20,w}$ [j]		+ 1.5	− 0.95[k]	+ 0.8[k]	+ 0.6[k]
$(\Delta s^c_{20,w})_{corr.}$ [l]		+ 3.9	+ 1.4		+ 3.0

[a] Abbreviations: CS, pig-heart citrate synthase; MS, yeast malate synthase
[b] Model parameters for CS are based on the prolate ellipsoidal models (PE)
[c] Model parameters for MS are based on the oblate ellipsoidal models (OE); the values in parentheses refer to the refined models (cf. Tables 5 and 7)
[d] The values refer to the models
[e] Percent change of the long semiaxis c
[f] Percent change of the semiaxis a
[g] Based on the anhydrous volume
[h] Based on an assumed hydration $\delta_1 = 0.35$ g/g [47]
[i] Sedimentation runs were performed at the following ligand concentrations: 10 mM oxaloacetate or glyoxylate or pyruvate, 1 mM AcCoA
[j] $s_{20,w}$ values are corrected for temperature and viscosity of the buffer, however neglecting the influence of ligands
[k] Taken from [34]
[l] $s_{20,w}$ values are corrected for temperature and viscosity of the buffer; additionally the influence of ligands on the partial specific volume of the protein and the density and viscosity of buffer was taken into account. The value determined experimentally for 10 mM oxaloacetate was also applied to the same concentration of glyoxylate or pyruvate; for 1 mM AcCoA no correction was used. No separation of the mass effects of the ligands was performed. Therefore, the given $\Delta s_{20,w}$ values represent the differences between the apoform (enzyme) and the holoform (enzyme plus bound ligand(s)). As may be taken from Table 1, the mass contribution of oxaloacetate, glyoxylate or pyruvate amounts only to 0.1–0.3% of the enzyme mass, while the mass of AcCoA is much greater (1.3%)

obtained when using the two approaches (Eqs. (20) or (21) and (22)) to determine the axial ratio p from the SAXS data. Furthermore the predictions for f/f_0, s and D are in accordance with the experimentally observed values for these quantities (Table 2). Reasonable estimates of hydrodynamic parameters from XD data (Table 6) can only be obtained if the hydration is taken into account.

As a consequence of binding oxaloacetate, our predictions from SAXS data imply an increase of $s_{20,w}$ by 3–4%. In agreement with this prediction, AUC also established an increase of this quantity (Table 3), however seemingly less pronounced (only $\simeq$ 1.5%). In covering all possibilities of corrections for $s_{20,w}$ (Table 8) the result is improved considerably (now $\simeq$ 4%). However, this approach requires a series of very accurate measurements, or qualified assumptions of minute changes occurring as a consequence of the presence of small amounts of ligands in the enzyme solutions and the solvent. The prediction of s values from XD data shows also increases of this quantity (Tables 6 and 8), precise predictions, however, are complicated by both the assumed value for protein hydration and the fact that there are slight deviations in overall shape between crystal and solution scattering data (cf. Table 4 and [33]).

Also in the case of malate synthase, the predictions for f/f_0, s and D values (Table 7) are compatible with the

experimental values (Table 2). As follows from the predictions, ligand binding to MS induces in each case minute increases of s (up to 2.8%). At the first glance, these predictions seem to contradict the experimentally observed changes of $s_{20,w}$ (cf. Table 3: Δs about -1% upon binding glyoxylate/pyruvate, $+0.8\%$ upon binding AcCoA, and about $+0.6\%$ upon formation of the ternary complex). Again, these discrepancies can be explained by correcting the s values with respect to the influences of the ligand concentration on η, ρ, and $\bar{v}$ (Table 8). For example, the decrease of 1% found for glyoxylate/pyruvate now turns to an increase of 1.4%.

Comparison of the results from different techniques

An inspection of Tables 3 to 8 discloses that all methods applied are capable of detecting small, but significant conformational changes occurring as a consequence of ligand binding, both in the overall structure and the local structure. Regarding the local structure, the spectroscopic data reveal alterations of intrinsic chromophores and fluorophores in their specific environment (with the secondary structure unchanged). On the other hand, insight into changes in the overall structure may be gained from results of sedimentation velocity experiments and small-angle scattering data. They can be compared quantitatively, provided all possible corrections for $s_{20,w}$ values are taken into account (Table 8). Considering reasonable degrees of hydration, the results of x-ray diffraction may be included in the comparison. Slight deviations between solution and crystal structures, however, may restrict the unconfined use of crystal data for this purpose. On the other side, the agreement between the two solution methods, AUC and SAS, is of great promise.

Evidence for the above-mentioned contributions of hydration also follows from the following considerations: The experimentally observed ratios of about $1.8 \times 10^{-3}\,\mathrm{nm^3 \cdot mol/g}$ for V/M and about $7.8 \times 10^{-2}\,\mathrm{nm^2 \cdot mol^{2/3}/g^{2/3}}$ for $S/M^{2/3}$ for the two synthases (Tables 4 and 5) corr espond to the amount of hydration (about 0.35 g/g) often found with different techniques including SAXS [26, 47, 77]. This is in fair accord with the values of about $1.96 \times 10^{-3}\,\mathrm{nm^3 \cdot mol/g}$ and $9.5 \times 10^{-2}\,\mathrm{nm^2 \cdot mol^{2/3}/g^{2/3}}$ given by Kumosinski and Pessen [25–27] as mean value for about 20 proteins, while the corresponding ratios for diffraction data reported by Teller [15] are $1.27 \times 10^{-3}\,\mathrm{nm^3 \cdot mol/g}$ and $11.1 \times 10^{-2}\,\mathrm{nm^2 \cdot mol^{2/3}/g^{2/3}}$. Obviously SAXS yields consistently higher volumes than XD, whereas the surface area in solution is slightly lower than the crystallographically accessible surface area. For $(S/V) \cdot M^{1/3}$ ratios (cf. [15]) the differences between SAXS and XD data are still more pronounced. Using the above values for $S/M^{2/3}$ and V/M, we obtain about $43\,\mathrm{nm^{-1} \cdot g^{1/3} \cdot mol^{-1/3}}$ for $(S/V) \cdot M^{1/3}$, again in reasonable agreement with a value of $48\,\mathrm{nm^{-1} \cdot g^{1/3} \cdot mol^{-1/3}}$ derived from the data of Kumosinski and Pessen [25–27]. Both values, however, are substantially lower than the value of $88\,\mathrm{nm^{-1} g^{1/3} \cdot mol^{-1/3}}$ derived from crystal data [15]. Discrepancies between SAXS and XD data have been ascribed to solvation effects and rugosities (surface roughness), electrostriction of proteins upon crystallization, as well as differences in the behavior of monomeric and oligomeric proteins [25–27]. Obviously in SAXS studies a protein volume is found which is higher by a factor of about 1.5 than the crystallographic volume; this is obviously caused by the formation of a hydration shell in solution. On the other hand, the protein surface area observed by SAXS is lower by a factor of approximately 1.3 as compared to XD; this is presumably due to the fact that the binding of solvent results in less anisotropy and/or less rugosity. Consequently, S/V ratios observed with the SAXS method are smaller than the crystallographically registered quantities. Different extents of hydration to monomeric and oligomeric proteins (according to Kumosinski and Pessen [26, 27] 0.280 and 0.444 g/g as appropriate averages) may hold as explanation for slightly different results observed for monomers and oligomers, respectively.

In this context it should be stressed that different experimental conditions and assumptions had to be used for SAXS and AUC experiments: for example, sedimentation runs are usually performed at concentrations of protein and ligands lower by a factor of about 10–100. While the results from SAXS might be perturbed by the presence of small amounts of aggregates, the centrifuge is spinning down these aggregates very rapidly.

The good accordance of the data found for the two solution techniques, therefore, clearly points to the registration of true conformational changes in the enzymes. In the case of low-mass contributions of ligands like oxaloacetate, glyoxylate or pyruvate, the results clearly rule out that the observed overall effects are merely caused by the mass of the ligand. On the other hand, the effects observed in the presence of AcCoA or CoA contain increments of both anisometry and mass. In summary, the major part of the effects is caused by conformational changes in the protein moieties.

Comparing the effects observed for dimeric citrate synthase and trimeric malate synthase (Table 8), the following conclusions can be drawn:

Upon ligand binding, both citrate synthase and malate synthase show a contraction of the enzyme as well as an increase in isometry. For both enzymes the effects found by SAXS or sedimentation analysis are small, but significant; they are quite different for the two enzymes,

obviously due to different shapes. When comparing the effects on a percentage basis, one has to recall that malate synthase has nearly double the size of citrate synthase (cf. Table 1). Correspondingly, ligand-induced percent changes of the gross structure in the case of malate synthase are expected to be less pronounced.

For example, for the binary complex of citrate synthase with oxaloacetate the following percent changes were observed: $R_G = -3.8\%$ and $s_{20,w} = +3.9\%$; however, for the complex of malate synthase with glyoxylate or pyruvate, the corresponding result is only $R_G = -1.3\%$ and $s_{20,w} = +1.4\%$ (Table 8). The small ligands (oxaloacetate on the one side, and glyoxylate/pyruvate on the other) turn out to be the major triggers of the structural changes. This confirms the crystallographic result that oxaloacetate is primarily responsible for the domain closure of citrate synthase [1, 50, 66].

The effects of AcCoA are less prominent than those observed for the small ligands; again the changes observed for citrate synthase exceed those for malate synthase (Tables 3 and 8). The different behavior of AcCoA when bound to these two synthases clearly rules out that the observed effects are only mass effects. In the case of malate synthase, the combined effects of both substrates exceed the contributions of the individual substrates. Apart from the changes in ellipticity at 260 nm, this could not be detected in the case of citrate synthase.

The percent changes of the spectroscopic signals were found to be significantly larger than the differences observed by hydrodynamic and solution scattering techniques; again, they differ for the two enzymes. In general, the comparison of the effects for citrate synthase and malate synthase clearly shows that, albeit similar in enzyme mechanism, the conformational changes accompanying ligand binding reflect the individual properties of the two enzymes. Of course, spectroscopy only gives indirect evidence for alterations of the overall structure of the enzyme molecules.

Denaturation studies of citrate synthase

Denaturation and dissociation of citrate synthase by extremes of pH, guanidinium chloride or urea were monitored by ultracentrifugal and spectroscopic analyses. While acid denaturation indicated only incomplete unfolding, denaturation by urea or guanidinium chloride was more effective: $s_{20,w} = 3.2$ S at pH 2, 1.7 S in 8 M urea, and 1.6 S in 6 M GdmCl, corresponding to $s_{20,w}$ changes of -48, -73 and -74%, respectively, when compared to the native enzyme (6.2 S). Correspondingly, the spectral signals changed in a manner typical of unfolded proteins (pronounced red shift of fluorescence emission maxima,

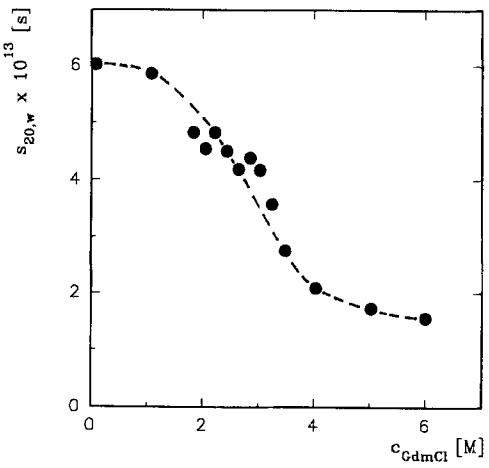

Fig. 2 GdmCl-dependent denaturation transition of citrate synthase, as monitored by determinations of sedimentation coefficients of the enzyme at varying denaturant concentrations

decrease of helix content, etc., in addition to enzyme deactivation).

The progress of unfolding was followed by measuring transition curves at different denaturant concentrations. The enzyme is nearly completely unfolded at > 4 M GdmCl. Spectroscopic and hydrodynamic techniques are complementary, rendering information on the state of protein chromophores and overall size and shape of the molecule under denaturing conditions. The spectroscopic techniques (EM, EX, CD) turned out to give relatively smooth curves, which allowed the determination of transition points ($c_{1/2}$). The evaluation of sedimentation velocity experiments, however, was complicated by the heterogeneity of the sample in the transition range (Fig. 2). Nevertheless, the transition point, $c_{1/2} = 2.5$ M GdmCl, coincides for the previously mentioned techniques. The substrate oxaloacetate (1 mM) stabilizes the enzyme to some extent against the deleterious effect of the denaturant, shifting the transition point to $c_{1/2} = 3$ M GdmCl. The results supplement earlier denaturation studies [62, 68, 72, 78]. As far as the protective effect of oxaloacetate is concerned, they confirm the behavior observed by Srere in the case of urea denaturation [68, 72]; this author, however, could not find indications for a protection in the case of GdmCl denaturation [68].

Concentration-dependent changes of malate synthase

Previous investigations have indicated a concentration-dependent deactivation behavior of malate synthase upon high dilution [34]. The specific activity decreased at a concentration $c_0 < 0.5$ mg/ml to reach a constant value of

activity. The deactivation was accompanied by structural changes, indicating concomitant dissociation. Structural alterations, however, occurred at different protein concentrations: s, M showed a decrease at $c < 0.1$ mg/ml, while the spectral signals (F, $[\theta]$) showed alterations already at $\simeq 2$ mg/ml. It is obvious that the techniques applied register shape changes with different sensitivity.

We reexamined the earlier findings, with the result that under reducing conditions unperturbed results could be achieved. Addition of DTT to already deactivated enzyme led to an enhancement of enzymic activity. Since malate synthase is known to possess essential sulfhydryl groups [76], this explanation seems to be conclusive. In this context it should also be mentioned that the activity of x-ray damaged malate synthase, which had been attacked by the radiolysis products of water as a consequence of irradiation of aqueous enzyme solutions, could be restored partly by DTT [76, 79]. The integrity of the enzyme sulfhydryls obviously turns out to be a necessary prerequisite for maintaining unchanged enzyme function and structure. This was demonstrated convincingly by monitoring both enzyme activity and overall-structural characteristics (s

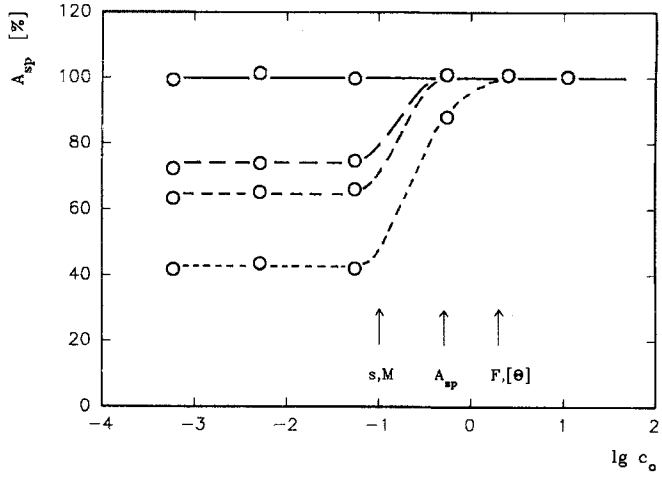

Fig. 3 Concentration-dependent changes of the enzymatic activity of malate synthase. Experiments were performed with enzyme solutions of varying protein concentration, c_0 (in mg/ml), different concentrations of DTT, c_{DTT}, and at different time intervals after protein dilution; in the assay, c_0 and c_{DTT} decrease by a factor of 150. ——: 10 mM freshly dissolved DTT, 30 min or 10 d; – –: 0.2 mM DTT, 30 min; – – –: 0.2 mM DTT, 24 h; - - - - -: 0.2 mM DTT, 10 d. With enzyme solutions containing insufficient amounts of reduced DTT, the specific activity, A_{sp}, decreases as a function of c_0 in the optical test, while in solutions containing elevated amounts of freshly dissolved (reduced) DTT obviously such changes do not occur. This peculiar behavior is confirmed by physico-chemical techniques: the arrows indicate where ultracentrifugal and spectroscopic techniques start monitoring changes of the observed quantities (s, M, F and $[\theta]$), provided the solution is devoid of significant amounts of reduced DTT

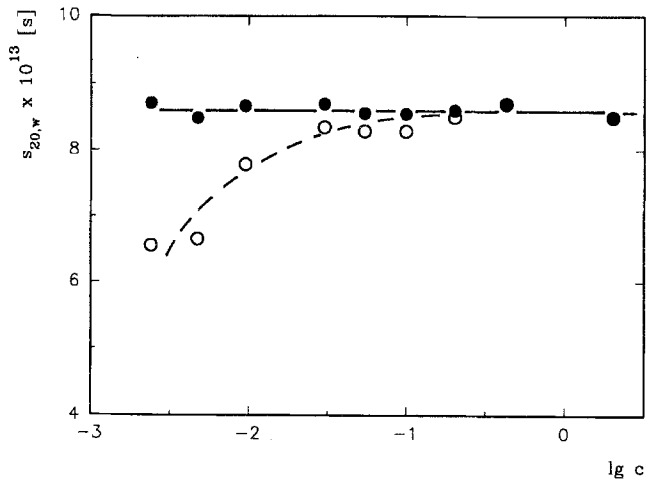

Fig. 4 Concentration-dependent change of the sedimentation coefficient of malate synthase. Sedimentation velocity experiments in buffer containing 0.2 mM DTT (○) reveal a decrease of s at $c < 0.1$ mg/ml, while in the presence of 1 mM fresh DTT (•) s remains constant

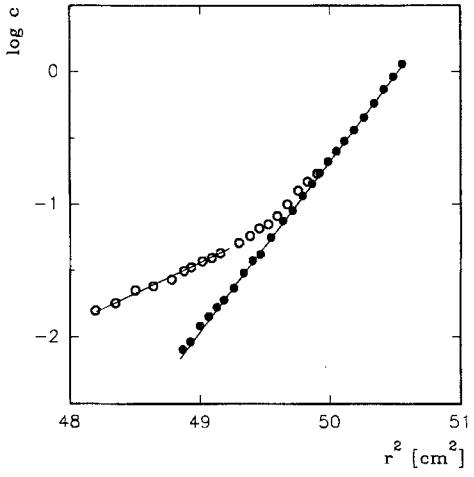

Fig. 5 Concentration-dependent change of the molar mass of malate synthase. High-speed sedimentation equilibrium experiments (16000 rpm, $c_0 = 1$ mg/ml) in buffer containing no or 0.2 mM DTT (○) give evidence of a dissociation of the trimeric protein to the monomer at $c < 0.1$ mg/ml (188 000 ± 5000 g/mol near the bottom of the cell, and 64 000 ± 2000 g/mol near its meniscus), while in the presence of 1 mM fresh DTT (•) no dissociation is observed

and M), in the absence and in the presence of sufficient amounts of DTT.

In the absence of reduced DTT, the enzyme deactivates to a constant level, activity decreasing further upon storage of the diluted enzyme (Fig. 3). The enzyme is stable, however, showing unchanged specific activity even at very high dilution, provided its sulfhydryls are protected effectively by another thiol (freshly dissolved DTT). The investigation of the sedimentation coefficient (Fig. 4) and molar mass (Fig. 5) reflect similar features. Both quantities

decrease in enzyme solutions devoid of sufficient amounts of reduced DTT, presumably due to a partial dissociation of the enzyme to the monomeric form. Having added freshly dissolved DTT to enzyme solutions of $c > 0.5$ mg/ml, neither the sedimentation coefficient nor the molar mass reveal any change of mass or shape over a wide range of enzyme concentrations. In this context it should be mentioned that also the presence of AcCoA + pyruvate prevents the enzyme from dissociation to the monomer. Presumably the conformational change occurring upon binding both ligands and/or shielding effects prevent the enzyme from dissociation. Again, this finding is in accordance with the fact that malate synthase contains essential sulfhydryl groups.

Conclusions

The present investigation shows that the study of small conformational changes by means of AUC or other physico-chemical techniques has to be performed with great care considering precautions with respect to the effects of altered solvent conditions on all relevant hydrodynamic, scattering and spectral parameters. It is absolutely indispensible to make use of different techniques when decisions concerning small conformational changes are to be made. This holds especially if relevant statements on the kind of alterations with respect to changes in mass, anisometry and/or hydration are intended. In interpreting the results one has to be aware of the specific complications connected with each of the techniques employed. In the study of large structural changes the situation is much more straightforward; however, the occurrence of heterogeneity in the samples and the superposition of different effects may also in this case furnish the results with a serious flaw.

Using SAXS and/or XD data, sedimentation and diffusion coefficients as well as frictional ratios and Stokes radii may be predicted. Knowledge of Stokes radii is of interest also for other types of hydrodynamic analyses such as size-exclusion chromatography. Consistency between hydrodynamic and SAXS data can also be assumed in the case of the small changes in the shape of protein molecules occurring on ligand binding.

Understanding solution structural parameters, which are sensitive to surface characteristics, is a necessary prerequisite for comparing and interpreting results obtained by different solution techniques. The calculation of hydrodynamic parameters from x-ray data can provide insight concerning hydration, molecular surface roughness, volume contraction, ambiguities regarding the contributions of shape and hydration to the frictional ratio, discrepancies between solution and crystal structural data, etc. Evidently, this offers important advantages in understanding the behavior of proteins in solution.

Acknowledgements The authors are much obliged to F. Bogner, K. Goldmann, S. Wenzl, and R. Wilfing for establishing the basis of some of the earlier experimental results.

References

1. Remington S, Wiegand G, Huber R (1982) J Mol Biol 158:111–152
2. Wiegand G, Remington S, Deisenhofer J, Huber R (1984) J Mol Biol 174:205–219
3. Polson A (1950) J Phys Colloid Chem 54:649–652
4. Mandelkern L, Flory PJ (1952) J Chem Phys 20:212–214
5. Scheraga HA, Mandelkern L (1953) J Am Chem Soc 75:179–184
6. Polson A (1967) Biochim Biophys Acta 140:197–200
7. Squire PG, Himmel ME (1979) Arch Biochem Biophys 196:165–177
8. Young ME, Carroad PA, Bell RL (1980) Biotechnol Bioeng 22:947–955
9. Dang CV, Dang CV (1983) Biochem Biophys Res Commun 117:464–469
10. Tyn MT, Gusek TW (1990) Biotechnol Bioeng 35:327–338
11. Müller JJ (1991) Biopolymers 31: 149–160
12. Perrin F (1934) J Phys Radium, Série VII, 5:497–511
13. Perrin F (1936) J Phys Radium, Série VII, 7:1–11
14. Kirkwood JG (1954) J Polym Sci 12:1–14
15. Teller DC (1976) Nature (London) 260:729–731
16. Teller DC, Swanson E, De Haën C (1979) Meth Enzymol 61:103–124
17. García de la Torre J, Bloomfield VA (1981) Quart Rev Biophys 14:81–139
18. García de la Torre J (1989) In: Harding SE, Rowe AJ (eds) Dynamic Properties of Biomolecular Assemblies. Royal Society of Chemistry, Cambridge UK, pp 3–31
19. García de la Torre J (1992) In: Harding SE, Rowe AJ, Horton JC (eds) Analytical Ultracentrifugation in Biochemistry and Polymer Science. Royal Society of Chemistry, Cambridge UK, pp 333–345
20. García de la Torre J, Navarro S, Lopez Martinez MC, Diaz FG, Lopez Cascales JJ (1994) Biophys J 67:530–531
21. Harding SE (1989) In: Harding SE, Rowe AJ (eds) Dynamic Properties of Biomolecular Assemblies. Royal Society of Chemistry, Cambridge UK, pp 32–56
22. Byron O (1995) In: Behlke J (ed) Abstracts of the IX Symposium on Analytical Ultracentrifugation. Max-Delbrück-Centrum für Molekulare Medizin, Berlin-Buch, p 24
23. Glatter O, Kratky O, eds (1982) Small Angle X-ray Scattering. Academic Press, London
24. Durchschlag H (1993) In: Baianu IC, Pessen H, Kumosinski TF (eds) Physical Chemistry of Food Processes, Vol 2: Advanced Techniques, Structures, and Applications. Van Nostrand Reinhold, New York, pp 18–117

25. Kumosinski TF, Pessen H (1982) Arch Biochem Biophys 219:89–100
26. Kumosinski TF, Pessen H (1985) Meth Enzymol 117:154–182
27. Pessen H, Kumosinski TF (1993) In: Baianu IC, Pessen H, Kumosinski TF (eds) Physical Chemistry of Food Processes, Vol 2: Advanced Techniques, Structures, and Applications. Van Nostrand Reinhold, New York, pp 274–306
28. Müller JJ, Damaschun H, Damaschun G, Gast K, Plietz P, Zirwer D (1984) Stud Biophys 102:171–175
29. Müller JJ, Pankow H, Poppe B, Damaschun G (1992) J Appl Cryst 25:803–806
30. Durchschlag H, Biedermann G, Eggerer H (1981) Eur J Biochem 114:255–262
31. Zipper P, Durchschlag H (1978) Eur J Biochem 87:85–99
32. Wilfing R (1985) Thesis, Univ Graz, Austria
33. Durchschlag H, Zipper P, Wilfing R, Purr G (1991) J Appl Cryst 24:822–831
34. Durchschlag H, Goldmann K, Wenzl S, Durchschlag G, Jaenicke R (1977) FEBS Lett 73:247–250
35. Purr G (1989) Diplomarbeit, Univ Regensburg, Germany
36. Weitzman PDJ, Danson MJ (1976) Curr Top Cell Regul 10:161–204
37. Yphantis DA (1964) Biochemistry 3: 297–317
38. Zipper P, Durchschlag H (1978) Z Naturforsch 33c:504–510
39. Durchschlag H, Jaenicke R (1983) Int J Biol Macromol 5:143–148
40. Durchschlag H (1986) In: Hinz H-J (ed) Thermodynamic Data for Biochemistry and Biotechnology. Springer-Verlag, Berlin-Heidelberg-New York-Tokyo, pp 45–128
41. Chervenka CH (1973) A Manual of Methods for the Analytical Ultracentrifuge. Spinco Division of Beckman Instruments, Palo Alto
42. Van Holde KE (1975) In: Neurath H, Hill RC (eds) The Proteins, Vol 1, 3rd ed. Academic Press, New York – San Francisco – London, pp 225–291
43. Harding SE, Rowe AJ, Horton JC, eds (1992) Analytical Ultracentrifugation in Biochemistry and Polymer Science. Royal Society of Chemistry, Cambridge UK
44. Jaenicke R (1964) In: Rauen HM (ed) Biochemisches Taschenbuch, II. Teil, 2nd ed. Springer-Verlag, Berlin–Göttingen–Heidelberg–New York, pp 746–767
45. Durchschlag H (1989) Colloid Polym Sci 267:1139–1150
46. Tanford C (1961) Physical Chemistry of Macromolecules, John Wiley & Sons, New York – London – Sydney
47. Cantor CR, Schimmel PR (1980) Biophysical Chemistry, Part II: Techniques for the Study of Biological Structure and Function. WH Freeman and Co, San Francisco, pp 555 and 586
48. Luzzati V, Witz J, Nicolaieff A (1961) J Mol Biol 3:367–378
49. Huber R (1987) Biochem Soc Transactions 15:1009–1020
50. Bennett WS, Huber R (1984) CRC Crit Rev Biochem 15:291–384
51. Durchschlag H, Zipper P (1994) Progr Colloid Polym Sci 94:20–39
52. Eisenberg H (1976) Biological Macromolecules and Polyelectrolytes in Solution. Clarendon Press, Oxford
53. Eisenberg H (1981) Q Rev Biophys 14:141–172
54. Durchschlag H, Jaenicke R (1982) Biochem Biophys Res Commun 108: 1074–1079
55. Schmid FX (1989) In: Creighton TE (ed) Protein structure, a practical approach. IRL Press at Oxford University Press, Oxford–New York–Tokyo, pp 251–285
56. Jaenicke R (1987) Prog Biophys Molec Biol 49:117–237
57. Jaenicke R, Rudolph R (1989) In: Creighton TE (ed) Protein structure, a practical approach. IRL Press at Oxford University Press, Oxford – New York – Tokyo, pp 191–223
58. Pace CN, Shirley BA, Thomson JA (1989) In: Creighton TE (ed) Protein structure, a practical approach. IRL Press at Oxford University Press, Oxford – New York – Tokyo, pp 311–330
59. Jaenicke R, Lehle K (1991) Progr Colloid Polym Sci 86:23–29
60. Creighton TE (1993) Proteins, Structures and Molecular Properties, 2nd ed WH Freeman and Co, New York.
61. Bloxham DP, Parmelee DC, Kumar S, Wade RD, Ericsson LH, Neurath H, Walsh KA, Titani K (1981) Proc Natl Acad Sci USA 78:5381–5385
62. Wu J-Y, Yang JT (1970) J Biol Chem 245:212–218
63. Durchschlag H, Purr G, Jaenicke R, Zipper P (1993) Progr Colloid Polym Sci 93:222–223
64. Srere PA (1972) Curr Top Cell Regul 5:229–283
65. Weitzman PDJ (1989) In: Hervé G (ed) Allosteric Enzymes. CRC Press, Boca Raton, pp 175–188
66. Wiegand G, Remington SJ (1986) Ann Rev Biophys Biophys Chem 15:97–117
67. Beeckmans S (1984) Int J Biochem 16:341–351
68. Srere PA (1966) J Biol Chem 241: 2157–2165
69. Singh M, Brooks GC, Srere PA (1970) J Biol Chem 245:4636–4640
70. Kollmann-Koch A, Eggerer H (1989) Eur J Biochem 185:441–447
71. Bayer E, Bauer B, Eggerer H (1981) Eur J Biochem 120:155–160
72. Srere PA (1965) Arch Biochem Biophys 110:200–204
73. Johansson C-J, Pettersson G (1979) Eur J Biochem 93:505–513
74. Eggerer H, Klette A (1967) Eur J Biochem 1:447–475
75. Clark JD, O'Keefe SJ, Knowles JR (1988) Biochemistry 27:5961–5971
76. Durchschlag H, Zipper P (1981) Z Naturforsch 36c:516–533
77. Pessen H, Kumosinski TF (1985) Meth Enzymol 117:219–255
78. West SM, Kelly SM, Price NC (1990) Biochim Biophys Acta 1037:332–336
79. Durchschlag H, Zipper P (1985) Radiat Environ Biophys 24:99–111